Arab J Sci Eng (2016) 41:4531–4552
DOI 10.1007/s13369-016-2160-0

RESEARCH ARTICLE - MECHANICAL ENGINEERING

Comparative Assessment on Machinability Aspects of AISI 4340 Alloy Steel Using Uncoated Carbide and Coated Cermet Inserts During Hard Turning

Anshuman Das[1] · **Akash Mukhopadhyay**[2] · **S. K. Patel**[2] · **B. B. Biswal**[1]

Received: 14 September 2015 / Accepted: 14 April 2016 / Published online: 14 May 2016

Abstract This paper compares the performances of uncoated carbide and coated cermet inserts for varied machinability aspects throughout the machining of hardened steel (AISI 4340, 48 HRC) in the dry cutting surroundings. Cutting speed, feed, and depth of cut were thought of as major governing parameters. Workpiece surface temperature, machining forces, and tool flank wear were taken as measures to check the performance estimation of various cutting inserts during this work. All the three input variables were ascertained to possess influence over workpiece surface temperature, feed, and radial force in case of uncoated carbide and cermet. Cermets exceeded the performance of carbides for flank wear, cutting force, and workpiece surface temperature, although carbides outperformed cermets concerning feed and radial force. The depth of cut was found to be the most vital, once feed and cutting forces were involved, whereas it had been true for radial force using carbides. Cutting speed affected workpiece surface temperature and flank wear for carbides the most; in the meantime, this was the same once considering the radial force with cermets. The feed was the foremost vital parameter, while the flank wear of cermets was taken into account. ANOVA, regression analysis, and main effect plots were accomplished using the MINITAB-16 software.

Keywords Hard turning · Hardened alloy steel · Flank wear · Cutting forces · Surface temperature of workpiece

List of symbols

ANOVA	Analysis of variance
AISI	American Iron and Steel Institute
CVD	Chemical vapor deposition
d	Depth of cut (mm)
DF	Degree of freedom
Eq.	Equation
f	Feed (mm/rev)
F_x	Axial/feed force (N)
F_y	Thrust/radial force (N)
F_z	Tangential/cutting force (N)
HRC	Rockwell hardness in C scale
K_f	Entering/approach angle (°)
L	Machining length (mm)
MQL	Minimum quantity lubrication
MS	Mean square
PVD	Physical vapor deposition
Pe	Peclet number
R-Sq	Coefficient of multiple determinations
r	Nose radius (mm)
SS	Sum of squares
SEM	Scanning electron microscope
SAE	Society of automotive engineers
T	Workpiece surface temperature (°C)
V	Cutting speed (m/min)
v	Cutting speed (m/s)
VBc	Flank wear of inserts (mm)
α	Thermal diffusivity (m^2/s)
α_o	Clearance angle (°)
γ_o	Rake angle (°)

✉ Anshuman Das
anshuman.das2009@gmail.com

[1] Department of Industrial Design, NIT Rourkela, Odisha 769008, India

[2] Department of Mechanical Engineering, NIT Rourkela, Odisha 769008, India

1 Introduction

In recent days, hard turning is being often preferred over the grinding operation as it consumes less time, cost, and energy. Figure 1 shows various causes affecting the performance of hard turning in the form of an Ishikawa cause and effect diagram. Advanced cutting inserts like carbide, cermet, ceramic, cubic boron nitride (CBN), polycrystalline cubic boron nitride (PCBN), and polycrystalline diamond (PCD) are suggested for use in hard machining in dry condition for attaining higher productivity [1].

Machining of workpiece material having hardness up to 45 HRC is known as soft machining. On the other hand, machining of the workpiece having a hardness in between 45 and 70 HRC comes under the category of hard machining. Use of cutting fluids in machining often results in occupational hazards [2]. Hence, it has motivated many researchers to investigate in different machinability aspects under dry conditions. In addition, there is a significant economic benefit as a result of non-usage of coolants. Machining of hard material in a dry environment is often recommended to be done at comparatively higher cutting speed because it results in a higher tool tip temperature, thereby softening the work piece material. Pal et al. [3] observed that harder work pieces resulted in higher cutting forces and higher tool–chip interface temperature but lower surface roughness. Further, surface roughness was most prominently affected by feed rates, whereas radial forces were affected by the depth of cut. Thus, cutting speed and depth of cut were more significant so far as tool–chip interface temperature is concerned. Suresh et al. [4] analyzed the effect of various process parameters on the machinability aspects in hard turning of AISI 4340 steel with multilayer coated carbide inserts. Their experiments showed that the tool wear mainly occurred due to abrasion and the machining power was mostly influenced by cutting speed. They also concluded that feed rate was the most significant parameter affecting machining force, specific cutting force, and surface roughness. The same conclusion was made by Selvaraj et al. [5] who optimized surface roughness, cutting force, and tool wear of nitrogen-alloyed duplex stainless steel during a

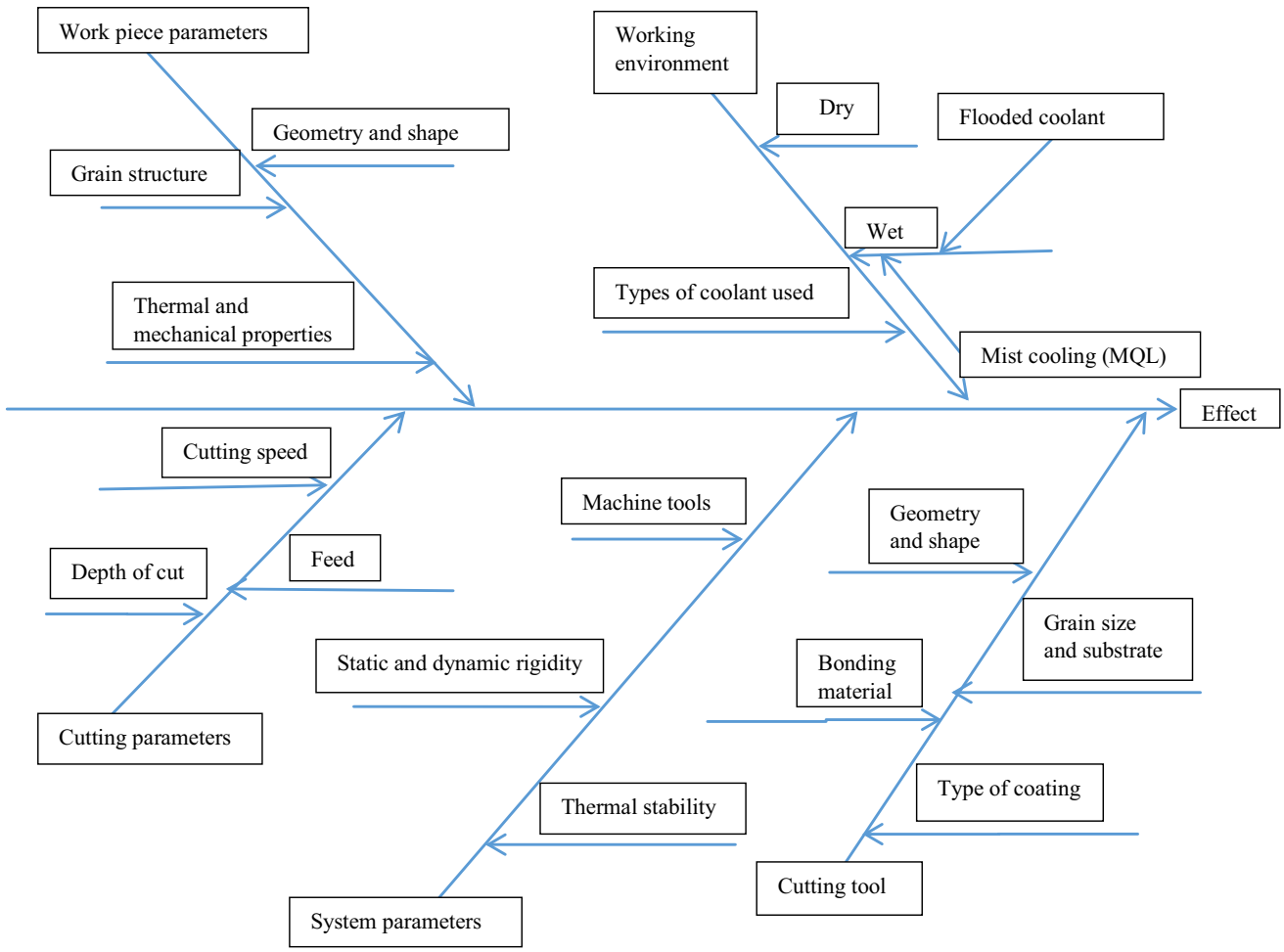

Fig. 1 Cause and effect diagram of hard turning

dry turning process using coated carbide inserts. They also resolved that cutting speed was the most significant parameter in tool wear. The tool wear was attributable to abrasion at lower cutting speeds, whereas at higher cutting speeds it is due to diffusion, thermal softening, and notching. Quazi et al. [6] also optimized cutting parameters in turning operation of mild steel, EN-8 and EN-31 steels using cermet inserts with grades of TN60, TP0500, and TT8020 for reducing surface roughness with the help of Taguchi's L_9 orthogonal array. They obtained minimum surface roughness in mild steel and EN-8 steel using TN60 tool and similarly in EN-31 steel using TT8020 tool. But, Sahoo and Sahoo [7] observed that chipping along with abrasion was responsible for tool wear in the hard turning of AISI 4340 steel using indexable multilayer coated carbide inserts. The surface finish was within the recommended range when using carbide inserts compared to cylindrical grinding. In addition, they observed that the color transformation of chips from metallic to burnt blue was much delayed using TiN-coated carbide inserts, and thus, these inserts should be preferred in hard machining. Further, they observed that thrust force was the largest component followed by tangential and feed forces. Reduction in cutting forces at higher cutting speed was also observed by them. Cutting speed and feed were the most notable parameters for both tool life and surface quality. Adesta et al. [8] showed an interesting result that there was a decrement in tool life and surface finish with an increase in negative rake angle. They found shorter tool life and better surface finish at higher cutting speed.

From experiments on AISI 4340 steel with single-layer physical vapor deposition (PVD)-coated and multilayer chemical vapor deposition (CVD)-coated carbide tools, Chinchanikar and Choudhury [9] observed that the tool–chip interface temperature increased rapidly with cutting speed, slightly with feed, but remained almost constant with the depth of cut. Moreover, the temperature was found to be greater in the case of CVD-coated tools than that of PVD-coated ones. The same authors reviewed various research articles on hard machining and concluded that majority of researchers have studied various machinability aspects of different materials with different tools under different cutting conditions, whereas the influences of the machining parameters on the quality and dimensional deviations of the product have not been studied thoroughly [10]. They claimed that many researchers have optimized machining parameters at a work piece hardness of 45–48 HRC, but very few work has been reported on optimization at 52 HRC or above. They also suggested numerous studies should be accomplished to discover the effects of various cutting fluids and different tool geometries on the machinability aspects of hardened steels.

Khan and Hajjaj [11] worked on the capabilities of TiN-coated cermet tools for high-speed machining of austenitic stainless steel. With the help of scanning electron microscope (SEM) images, they observed that the failure of cutting edges of cermet tools started with microcracks and these cracks grew gradually to cause the tool failure due to low fracture toughness. It gave satisfactory results to use cermet tools while machining at low values of all three machining parameters, viz., cutting speed, feed, and depth of cut. They recommended for keeping the cutting speed below 300 m/min, feed rate below 0.2 mm/rev, and depth of cut under 0.3 mm to have a satisfactory tool life. The similar recommendation was also suggested by Noordin et al. [12] who found the tool life of TiCN-based cermet inserts to be the highest at low cutting speed and low feed rate. However, the performance of coated carbides was superior at both medium and high values of cutting speed as well as feed. From the experimental results, they also observed that with an increase in negative side cutting edge angle, tool life increased. Ghani et al. [13] investigated on the wear mechanisms, in the end milling operation of AISI H13 tool steel using TiN-coated carbide and uncoated cermet inserts. They found that the tool wear phenomenon occurred predominantly in the form of flank wear. Besides, they determined that the time taken by coated carbides to initiate cracking and fracturing was more than that of the uncoated cermet. They also concluded that uncoated cermets experienced more uniform and gradual wear compared to coated carbides with the low values of speed, feed, and depth of cut. Ozkan et al. [14] provided a comparative analysis of the performance of coated carbide and cermet cutting tools in turning of 50CrV4 steel. The minimum and maximum values of surface roughness were obtained with cermet and carbide inserts, respectively. They also discovered that coated carbide tools resulted in maximum axial, radial, and cutting forces, whereas minimum values of respective three forces were attained with cermet inserts. Thoors et al. [15] performed dry turning operation on two variants of quenched and tempered steel and one ball bearing steel with the help of cermet and tungsten carbide-based inserts. Cermet tools were found to have low friction and wear resistance compared to carbide tools. Moreover, tool–chip contact stresses were different in different types of workpiece materials. Prevalent mechanisms of crater and flank wear in cermet tools were abrasion and adhesive types of damage in the machining of quenched and tempered steel, while plastic deformation, cracking, and occasional microchipping were the three major wear mechanisms in the case of bearing steel. Sert et al. [16] studied wear behavior of PVD TiAlN, CVD TiN-coated carbides, and uncoated cermet cutting tools in turning of AISI 5140 steel. The tool wear rate had a great effect on surface roughness and dimensional deviation. Based on experimental observations, they discouraged the use of uncoated cermet tools in machining of AISI 5140 steel at high cutting speed due to the high wear rate. They illustrated that TiN-coated inserts performed better than TiAlN-coated inserts in the higher cutting speed range. Chen

et al. [17] also investigated the cutting performance and wear characteristics of Ti (C, N)-based cermet while machining hardened steel at 61–63 HRC. The outcomes were compared with the multilayer coated carbide tools. Higher tool life of cermet was accomplished at a lower depth of cut. Adhesion, diffusion, and abrasion were three major wear mechanisms for both cermet and carbide tools. The lower surface finish was achieved by cermet compared to carbide. Severe crater wear was found for carbide due to adhesion and diffusion. Flank wear was critical for cermets. Wavy chips are found for both the cutting tools due to the generation of high temperature. Dosbaeva et al. [18] compared the performance of CVD-coated carbide tools with polycrystalline cubic boron nitride (PCBN) tools in hard turning of D2 steel at 52 HRC. The results revealed that carbide tool outperformed PCBN tool within a specific cutting condition. At lower cutting speed and corresponding cutting temperature, the tool life of carbide was greater than that of PCBN. But at higher cutting speed, the tool life of PCBN was higher compared to carbide. Primary wear mechanisms for PCBN tool were chemical and adhesion. Finally, they recommended that PCBN tool is a better option for high precision machining compared to carbide for its low wear rate.

Fnides et al. [19] evaluated the tool lives of various cutting materials, viz., carbides, ceramics, and cermets in the dry hard turning of AISI H11 steel, and the tool life was mostly affected by cutting speed. The tool lives of uncoated and coated cermet inserts were found to be the minimum (i.e., less than 2 min), whereas maximum tool life was obtained with mixed ceramic (i.e., 49 min). Moreover, Shalby et al. [20] examined the performances of three different types of tools, i.e., PCBN, coated PCBN, and mixed ceramic tools. They concluded that mixed ceramic tool outperformed both PCBN and coated PCBN tools in terms of tool life and machining forces. Instead of coating, there was no improvement in the tool life for PCBN tools. The major wear characteristics for PCBN tools were adhesion, abrasion, and diffusion. Hessainia et al. [21] studied the impacts of machining parameters and tool vibration on surface roughness and developed a statistical model. The authors also optimized the input variables to get desired surface finish while machining 42CrMo4 steel with the mixed ceramic tool. They found that surface roughness was highly influenced by feed rather than tool vibration. From the optimization results, they revealed that high speed, low feed, and low depth of cut would deliver better surface finish.

D'Errico et al. [22] used uncoated and TiN-, Ti (C, N)-coated cermet inserts with and without chamfered edge in continuous and interrupted turning operation of SAE 1045 steel. From the experimental results, they concluded that PVD-coated inserts without chamfered edge performed well only in continuous turning instead of interrupted turning. Moreover, they stated that tools with chamfered edge are better for interrupted turning where the high depth of cut was involved. There was no significant effect of coating on tool life, regardless of their cutting edges in interrupted turning. Rajabi et al. [23] summarized the investigations on the improvement of Ti(C)-based cermets. They found grain size and chemical composition of binders have a substantial effect on the toughness of Ti(C)-based cermets. They also found that instead of having different qualities, Ni binder is not much prominent because of its low wettability with ceramic particles. In this regard, Mo has been considered as a good binding material for Ti(C)-based cermets for its good wettability property.

The literature reveals that extensive research findings have been reported in the literature on hard machining of AISI 4340 alloy steel using carbide inserts, whereas limited work is found for the same using cermet inserts. Further, comparative analyses between the above-mentioned two types of inserts were found in the literature only in the case of stainless tool steels, alloy steel, ball bearing steel, and D2 steel, but the similar comparative study has not been found in AISI 4340 alloy steel at 48 HRC. Furthermore, the researchers have not studied the workpiece surface temperature as an output response.

In view of the above-mentioned research gap, the objective of the present work relies on the comparative analysis of uncoated carbides and multilayer coated cermets in hard turning of AISI 4340 alloy steel having a hardness of 48 HRC. The machining operation was carried out in dry circumstances, according to Taguchi's L_9 standard orthogonal array. The machinability aspects of the workpiece are investigated based on output responses like flank wear, work piece surface temperature, and machining forces. Analysis of variance (ANOVA) was conducted to identify the input parameters which significantly affect the specified responses. These responses were also fitted in the regression models with respect to the input variables and their interactions.

2 Experimental Details

Figure 2 shows the cylindrical bar of 50 mm diameter and 700 mm length made of AISI 4340 alloy steel which is used for the experiment.

Three parameters like cutting speed, feed, and depth of cut are varied at three levels throughout hard turning, and their influences on output responses like flank wear, workpiece surface temperature, and machining forces are examined. The experimental runs are designed in line with Taguchi's L_9 orthogonal array so as to save both time and cost as compared to a full factorial design without notably compromising the accuracy of results. Before beginning actual machining operation, the rough layers were first removed from the outer surface of the specimen to mitigate any consequences of

Fig. 2 Workpiece

non-uniformity on the output responses. Machining length was fixed at 300 mm for every experimental run. Readings of cutting, feed, and radial forces are recorded for every experimental run. The workpiece surface temperature was measured in three zones, i.e., 0–100, 100–200, and 200–300 mm of cutting length, and their mean has been evaluated. A specific cutting edge of the inserts was used for entire machining length in an experimental run. After each such trial, the flank wear of the insert was measured using an advanced optical microscope and its wear pattern was studied using scanning electron microscope (SEM).

2.1 Test Sample

AISI 4340 steel is hard to machine owing to excessive hardness, low specific heat, and high strain hardening. It is a low alloy steel comprising nickel, chromium, and molybdenum. It is often heat treated to increase its hardness. To improve the machinability, it is usually tempered after heat treatment. Thus, almost all standard machining processes can be possible on this material. The use of this type of steel is extremely widespread within the industry in the making of various components like gears, bearings, axles, and shafts. It may also be used as a material for numerous structures and aircraft elements. Table 1 shows the chemical composition of the specimen as observed using Spectro metal analyzer.

2.2 Heat Treatment

The sample was heated to an austenitizing temperature of 920 °C, i.e., higher than the upper critical temperature, where the solid solution of iron and carbon would exist. Once austenized, the workpiece was kept at that temperature for nearly 30 min, to execute the respective reformations within the crystalline structure, and then quenched in oil. After quenching the tempering was accomplished by reheating the specimen to a temperature of 400 °C (i.e., below the lower critical temperature) for 2 h followed by cooling in still air for getting rid of residual stresses to accumulate the homogeneous structure. After heat treatment, the hardness of the sample got increased from 18 HRC to 48 HRC as measured on the Rockwell hardness testing machine with an indentation at 150 kgf load by the sphero-conical diamond indenter.

Table 1 Chemical composition of specimen

Elements	Weight percentage
Carbon	0.397
Silicon	0.339
Manganese	0.770
Nickel	1.550
Chromium	0.900
Molybdenum	0.275

Fig. 3 Uncoated carbide with designated tool holder

2.3 Cutting Tools

In the present work, two types of cutting inserts are used, viz., uncoated carbides and multilayer PVD-coated cermets. Uncoated carbides are tungsten cobalt based which are designated by SNMG 120408. These inserts of grade K313 were procured from M/s Kennametal. The shape of each insert is square (90° point angle) without any specific type of chip breaker geometry. This insert is mounted on a tool holder of ISO designation PSBNR 2020K12 as shown in Fig. 3. The tool holder has the subsequent cutting geometries, i.e., clearance angle $= 0°$, back rake and side rake angles $= -6°$, entering angle $= 75°$, point angle $= 90°$, and nose radius $=$ 0.8 mm.

Constituents of cermet are ceramic particles with metallic binders. Cermet inserts utilized in this experiment are multilayer (TiN/TiCN/TiN) PVD coated. Such inserts of designation CNMG 120408 and grade KT315ff having a rhombic form (80° point angle) with fine finish chip breaker geometry as shown in Fig. 4 were procured from M/s Kennametal.

Fig. 4 Cermet insert

Fig. 5 Tool holder for cermets

Table 2 Nomenclature of inserts

Nomenclature	Details
S	Insert shape (90° point angle, square)
C	Insert shape (80° point angle, rhombic)
N	Clearance angle (0°)
M	Tolerance class [±0.002 for inscribed circle (d), ±0.003 for height of insert (m), ±0.0005 for thickness (s)]
G	Insert features—number of cutting edges with types of chip breaker geometry
12	Cutting edge length (12 mm)
04	Insert thickness (4.76 mm)
08	Nose radius (0.8 mm)

Figure 5 shows the tool holder utilized in this work that belongs to ISO designation PCLNR 2020K12 with clearance angle = 0°, back rake and side rake angles = −6°, entering angle = 95°, point angle = 80°, and nose radius = 0.8 mm.

For both the inserts nose radius and back rake angle are the same (i.e., 0.8 mm and −5°). Titanium nitride coatings were given at inner and outer most layers and titanium carbonitrides as an intermediate layer. The details of nomenclature of inserts are given in Table 2.

Figures 6 and 7 show the elemental analysis of the coated cermet insert and uncoated carbide insert, respectively. The percentages of elements present in the above two insert materials are shown in Tables 3 and 4, respectively. Both the sets of results match with that obtained from the supplier of these inserts.

2.4 Machine Tool and Measuring Instruments

Figure 8 shows the experimental setup. The turning operation was executed on a heavy duty lathe of HMT make with spindle power of 11 kW and in a cutting speed range of 40–2040 rpm. For measuring of cutting forces, three-dimensional dynamometer of make Kistler was used and the temperature was measured using an infrared thermometer. Flank wear of the inserts was analyzed using advanced optical microscope of model 100HD-3D (Carl Zeiss) and scanning electron microscope (JEOL JSM-6084 LV). Elemental analyses of both the inserts were done with the assistance of a Nova Nano field emission scanning electron microscope.

2.5 Cutting Conditions

Various machining conditions adopted during the experiment are shown in Table 5.

3 Results and Discussion

The results obtained from the experiments for uncoated carbide and coated cermets are shown in Tables 6 and 7, respectively. The abbreviations used in both these tables are same. For each of the nine experimental runs, the responses like three machining forces F_x, F_y and F_z, flank wear of the insert VBc, and workpiece surface temperature T are measured and shown in these tables. The corresponding three cutting parameters at which each experiment was conducted, viz., cutting speed V, feed f, and depth of cut d, are also mentioned. Since the temperature is measured in handheld infrared thermometer, to ensure the accuracy of the results, three readings are taken for each experimental run and their mean value is considered as mentioned in Tables 6 and 7. The bar charts showing 95 % confidence intervals for temperature readings in case of carbide and cermet are shown in Figs. 9 and 10.

These results are analyzed with the help of analysis of variance (ANOVA), multiple regression analysis, and main effect plots obtained using the MINITAB-16 software. The significance of input variables on responses is determined by ANOVA. The relationship between input and output parameters is established using multiple regression analysis. The results of both uncoated carbide and coated cermet have been graphically compared through main effect plots.

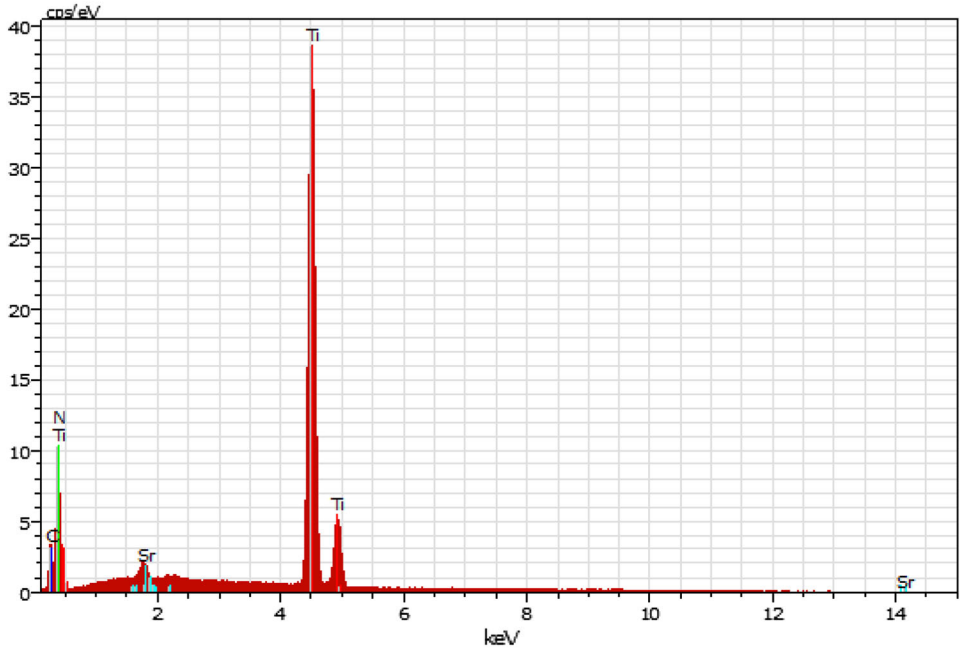

Fig. 6 Elemental analyses of coated cermet insert

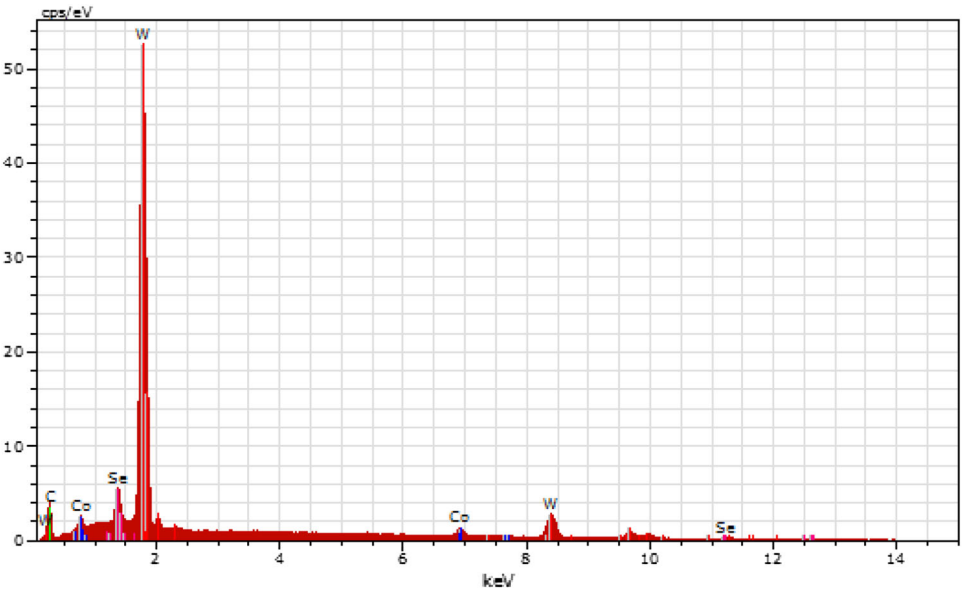

Fig. 7 Elemental analyses of uncoated carbide insert

Table 3 Percentage of elements in coated cermet insert

Element	Normalized C (wt%)	Atomic C (wt%)
Ti	77.91	51.17
N	15.14	34
C	5.46	14.3
Sr	1.49	0.54

Table 4 Percentage of elements in uncoated carbide insert

Element	Normalized C (wt%)	Atomic C (wt%)
W	83.07	30.06
C	11.52	63.84
Co	5.40	6.10
Se	1.98	0.73

3.1 Analysis of Variance

Analysis of variance is employed to observe the significance of machining parameters on the outcomes of the experiments. The results of ANOVA carried out at 5 % significance level are shown in Tables 8, 9, 10, 11, 12, 13, 14, 15, 16, and 17 for both cutting tools (i.e., uncoated carbide, coated cermet) and output responses (i.e., cutting force, feed

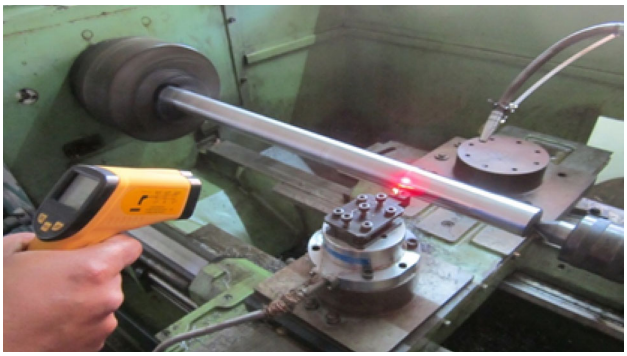

Fig. 8 Experimental setup for force and temperature measurement

Table 5 State of machining

Machining conditions	Descriptions
Workpiece material	AISI4340
Hardness	48 HRC
Cutting speed	80, 100, 120 m/min
Feed	0.05, 0.1, 0.15 mm/rev
Depth of cut	0.1, 0.2, 0.3 mm
Cutting environment	Dry
Cutting inserts	Tool 1: uncoated carbide (K313)
	Tool 2: multilayer coated cermet (KT315)
Tool geometry	SNMG 120408, CNMG120408
Tool holder	PSBNR 2020K12, PCLNR 2020K12
Machining length	300 mm
Output responses	Flank wear; feed, cutting, and radial forces; workpiece surface temperature

force, radial force, flank wear, and workpiece surface temperature). For each combination, the effects of three cutting parameters like cutting speed, feed, and depth of cut have been examined.

Tables 8, 9, and 10 reveal that all the three cutting parameters (i.e., cutting speed, feed, and depth of cut) are significantly affecting all three machining forces (i.e., cutting, feed, and radial forces) while machining with carbide insert, among which the depth of cut has the highest significance in all cases.

Table 11 shows that the cutting speed and depth of cut are the significant factors for the cutting force in case of coated cermet. For the same coated cermet, Table 12 shows that feed force is affected by the depth of cut with the highest significance followed by feed and cutting speed. Similarly, Table 13 indicates that all the three cutting parameters have significant effects on the radial force out of which cutting speed has the highest effect and depth of cut has the lowest effect.

It is observed from Table 14 that cutting speed is the sole dominant variable during experiments for the flank wear of the uncoated carbide. Table 15 shows that feed is the most significant factor affecting the flank wear of coated cermet followed by cutting speed and depth of cut.

It is found from Table 16 that cutting speed is the most significant factor on workpiece temperature while cutting with uncoated carbide. The impact of depth of cut is also significant, but it is comparatively less.

For coated cermet inserts, all three cutting parameters are significant for workpiece surface temperature out of which cutting speed and depth of cut are most & least significant as shown in Table 17.

Figure 11 shows the interaction plots in case of machining with carbide inserts obtained with the help of MINITAB-16. From the analysis of these plots, it is found that all the interactions of machining parameters are viable. Similar pattern of results is also obtained in case of coated cermets. Hence, while formulating the mathematical models, the impact of interaction effects must be considered. The multiple linear regression equations developed for each response in terms of three input cutting parameters along with their interactions are given below for both coated and uncoated inserts.

Table 6 Responses for uncoated carbide

Experimental run	V (m/min)	f (mm/rev)	d (mm)	F_x (N)	F_y (N)	F_z (N)	VBc (mm)	T (°C)
1	80	0.05	0.1	70	245	103	0.33000	27
2	80	0.10	0.2	165	490	270	0.52000	25
3	80	0.15	0.3	222	505	260	0.34710	38
4	100	0.05	0.2	121	280	224	0.80000	49
5	100	0.10	0.3	203	382	232	0.72000	56
6	100	0.15	0.1	72	236	90	0.32780	52
7	120	0.05	0.3	181	262	205	0.93830	60
8	120	0.10	0.1	78	211	85	0.77003	53
9	120	0.15	0.2	143	359	230	0.65000	50

Table 7 Responses for coated cermet

Experimental run	V (m/min)	f (mm/rev)	d (mm)	F_x (N)	F_y (N)	F_z (N)	VBc (mm)	T (°C)
1	80	0.05	0.1	133	463	97	0.19140	28
2	80	0.10	0.2	159	558	111	0.13110	27
3	80	0.15	0.3	197	632	150	0.11020	32
4	100	0.05	0.2	168	641	72	0.14110	36
5	100	0.10	0.3	196	705	98	0.05360	39
6	100	0.15	0.1	163	696	50	0.08170	26
7	120	0.05	0.3	192	708	111	0.17099	57
8	120	0.10	0.1	159	677	68	0.11300	42
9	120	0.15	0.2	189	758	86	0.14000	44

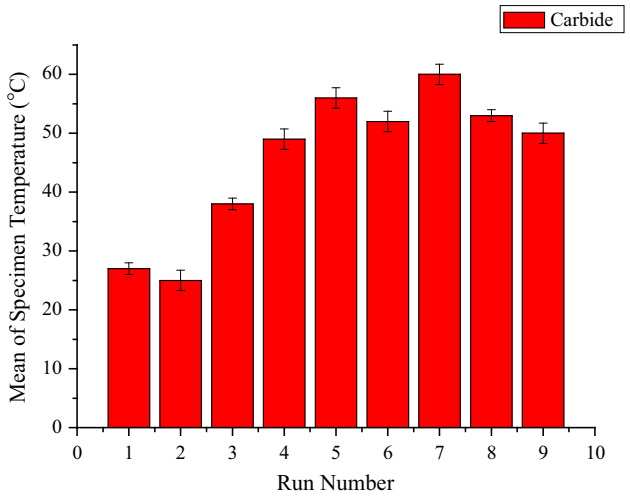

Fig. 9 Bar chart with specimen temperature variation (carbide)

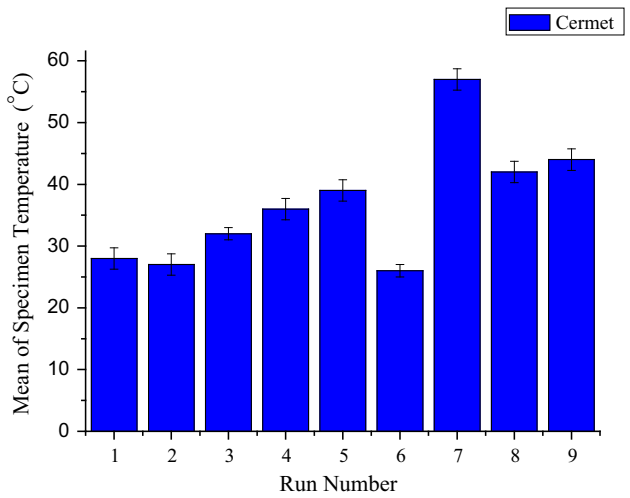

Fig. 10 Bar chart with specimen temperature variation (cermet)

3.2 Mathematical Modeling

For uncoated carbides:

$$F_z = 306.968 - 0.76619\ V - 6728.57\ f + 4803.33d + 13.4571\ V * f - 4.88571\ V * d - 8371.43\ f * d \quad R - \mathrm{Sq} = 83.23\,\%$$

$$F_x = 0.396825 - 0.0209524\ V - 476.19\ f - 0.928571\ V * d + 1253.33\ d + 1.08571\ V * f - 257.143\ f * d \quad R - \mathrm{Sq} = 97.99\,\%$$

$$F_y = 495.905 - 0.885714\ V - 5500.95\ f + 4880.95\ d + 11.7429\ V * f - 5.5\ V * d - 5257.14\ f * d \quad R - \mathrm{Sq} = 86.86\,\%$$

$$\mathrm{VBc} = -1.37462 + 0.00267195\ V - 13.3609\ f + 15.079d + 0.0233134\ V * f - 0.0184323\ V * d - 24.742\ f * d \quad R - \mathrm{Sq} = 98.70\,\%$$

$$T = -78.254 + 0.168095\ V + 341.905\ f + 238.095\ d - 0.285714\ V * f - 0.2\ V * d - 885.714\ f * d \quad R - \mathrm{Sq} = 81.58\,\%$$

For coated cermets:

$$F_z = 129.095 + 0.0857143\ V + 1734.29\ f - 1744.29\ d - 4.74286\ V * f + 2\ V * d + 6657.14\ f * d \quad R - \mathrm{Sq} = 90.18\,\%$$

$$F_x = 44.0317 + 0.112857\ V + 215.238\ f + 286.667\ d - 0.0571429\ V * f - 0.114286\ V * d - 28.5714\ f * d \quad R - \mathrm{Sq} = 98.38\,\%$$

$$F_y = -98.1905 + 0.669524\ V - 458.095\ f + 3163.33d + 4.94286\ V * f - 2.91429\ V * d - 9428.57\ f * d \quad R - \mathrm{Sq} = 96.57\,\%$$

$$\mathrm{VBc} = 0.508565 - 0.000186595\ V + 2.0041\ f$$

Table 8 ANOVA of cutting force with uncoated carbide

Source	DF	SS	MS	F	P	Remarks
V	2	2334.9	1167.4	656.69	0.002	Significant
f	2	597.6	298.8	168.06	0.006	Significant
d	2	41,689.6	20,844.8	11,725.19	0.000	Significant
Error	2	3.6	1.8			
Total	8	44,625.6				
$S = 1.333$		R-Sq = 100 %		R-Sq(adj) = 100 %		

Table 9 ANOVA of feed force with uncoated carbide

Source	DF	SS	MS	F	P	Remarks
V	2	753.6	376.8	178.47	0.006	Significant
f	2	1086.9	543.4	257.42	0.004	Significant
d	2	24,889.6	12,444.8	5894.89	0.000	Significant
Error	2	4.2	2.1			
Total	8	26,734.2				
$S = 1.453$		R-Sq = 100 %		R-Sq(adj) = 99.9 %		

Table 10 ANOVA of radial force with uncoated carbide

Source	DF	SS	MS	F	P	Remarks
V	2	31,976.0	15,988.0	1713.00	0.001	Significant
f	2	20,652.7	10,326.3	1106.39	0.001	Significant
d	2	44,468.7	22,234.3	2382.25	0.000	Significant
Error	2	18.7	9.3			
Total	8	97,116.0				
$S = 3.055$		R-Sq = 100 %		R-Sq(adj) = 99.9 %		

Table 11 ANOVA of cutting force with coated cermet

Source	DF	SS	MS	F	P	Remarks
V	2	3302.00	1651.00	61.15	0.016	Significant
f	2	14.00	7.00	0.26	0.794	Insignificant
d	2	3528.00	1764.00	65.33	0.015	Significant
Error	2	54.00	27.00			
Total	8	6898.00				
$S = 5.196$		R-Sq = 99.2 %		R-Sq(adj) = 96.9 %		

Table 12 ANOVA of feed force with coated cermet

Source	DF	SS	MS	F	P	Remarks
V	2	468.22	234.11	27.72	0.035	Significant
f	2	533.56	266.78	31.59	0.031	Significant
d	2	2820.22	1410.11	166.99	0.006	Significant
Error	2	16.89	8.44			
Total	8	3838.89				
$S = 2.906$		R-Sq = 99.6 %		R-Sq(adj) = 98.2 %		

$$T = -16.2698 + 0.119048\ V + 303.81\ f - 366.667\ d$$
$$-4.78528\ d - 0.00698486\ V * f + 0.00571957\ V * d \quad -0.914286\ V * f + 0.471429\ V * d$$
$$+10.934\ f * d \quad R - \mathrm{Sq} = 69.51\,\% \quad +1142.86\ f * d \quad R - \mathrm{Sq} = 98.53\,\%$$

Table 13 ANOVA of radial force with coated cermet

Source	DF	SS	MS	F	P	Remarks
V	2	44,624.7	22,312.3	199.22	0.005	Significant
f	2	12,530.7	6265.3	55.94	0.018	Significant
d	2	7340.7	3670.3	32.77	0.030	Significant
Error	2	224.0	112.0			
Total	8	64,720.0				
$S = 10.58$		$R - \text{Sq} = 99.7\,\%$		$R - \text{Sq(adj)} = 98.6\,\%$		

Table 14 ANOVA of flank wear with uncoated carbide

Source	DF	SS	MS	F	P	Remarks
V	2	0.225834	0.112917	28.34	0.034	Significant
f	2	0.113938	0.056969	14.30	0.065	Insignificant
d	2	0.069865	0.034933	8.77	0.102	Insignificant
Error	2	0.007970	0.003985			
Total	8	0.417607				
$S = 0.06313$		$R - \text{Sq} = 98.1\,\%$		$R - \text{Sq(adj)} = 92.4\,\%$		

Table 15 ANOVA of flank wear with coated cermet

Source	DF	SS	MS	F	P	Remarks
V	2	0.005143	0.002572	57.16	0.017	Significant
f	2	0.008107	0.004053	90.10	0.011	Significant
d	2	0.001034	0.000517	11.49	0.080	Insignificant
Error	2	0.000090	0.000045			
Total	8	0.014374				
$S = 0.006707$		$R - \text{Sq} = 99.4\,\%$		$R - \text{Sq(adj)} = 97.5\,\%$		

Table 16 ANOVA of specimen temperature with uncoated carbide

Source	DF	SS	MS	F	P	Remarks
V	2	1094.89	547.444	133.16	0.007	Significant
f	2	6.22	3.111	0.76	0.569	Insignificant
d	2	160.89	80.444	19.57	0.049	Significant
Error	2	8.22	4.111			
Total	8	1270.22				
$S = 2.028$		$R - \text{Sq} = 99.4\,\%$		$R - \text{Sq(adj)} = 97.4\,\%$		

Table 17 ANOVA of specimen temperature with coated cermet

Source	DF	SS	MS	F	P	Remarks
V	2	566.222	283.111	2548.00	0.000	Significant
f	2	62.889	31.444	283.00	0.004	Significant
d	2	176.222	88.111	793.00	0.001	Significant
Error	2	0.222	0.111			
Total	8	805.556				
$S = 0.3333$		$R - \text{Sq} = 100\,\%$		$R - \text{Sq(adj)} = 99.9\,\%$		

The parameter R square (R-Sq) evaluates the proximity of the responses with the fitted multiple regression lines. R-Sq is called as the constant of multiple determinations. If the regression equations predict the responses better and the fittings are proper, then R-Sq values come closer to 100 %. An equation with R-Sq value of 90 % will demonstrate a variability of 90 % in the dependent parameters.

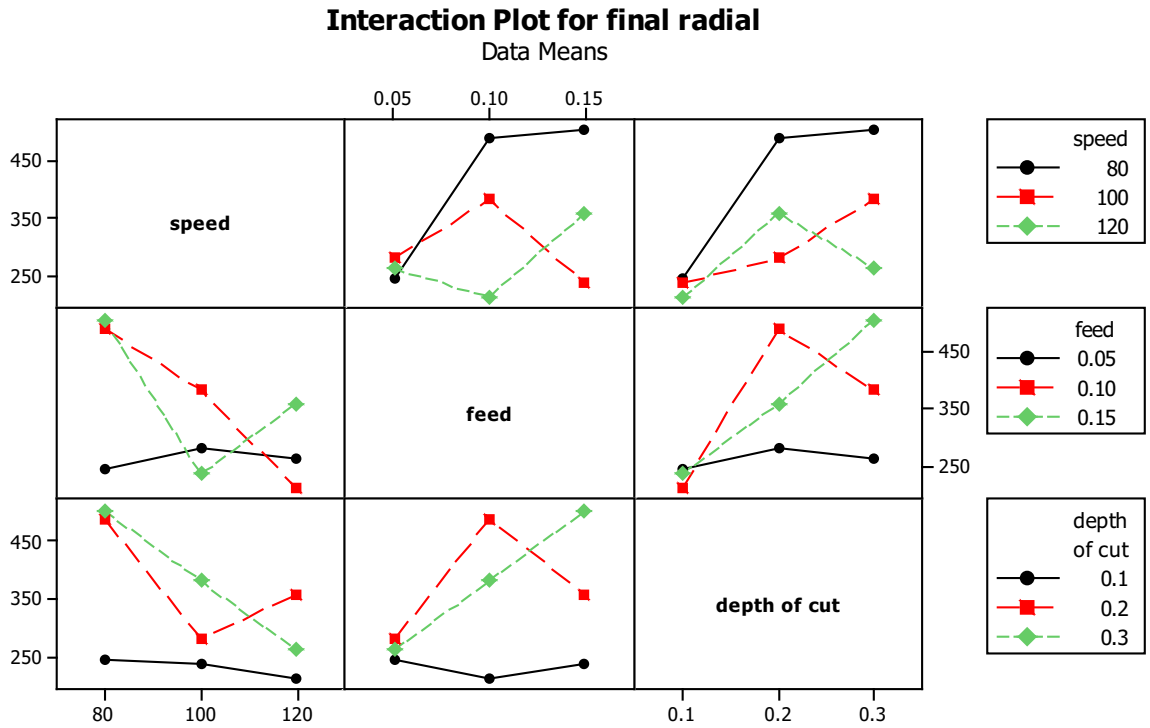

Fig. 11 Interaction plot for radial force using carbide inserts

3.3 Graphical Analysis

Comparisons of different responses for uncoated carbide and cermet insert are discussed with the aid of the following main effect plots for means of each response.

Figure 12a, b illustrates the main effect plots for cutting force using uncoated carbide and coated cermet. There is a decrease in cutting force when cutting speed changes from 80 to 100 m/min. However, it again increases for cermets up to 120 m/min. The cutting force remains nearly constant with feed for cermets and, however, enhances slightly for carbides with a change of feed from 0.05 to 0.1 mm/rev. There is a drastic increase in cutting force for carbides when the depth of cut increases from 0.1 to 0.2 mm and then decreases slightly. However, a steady increase in the cutting force with the depth of cut using cermets can be observed.

From Fig. 13a, b it is observed that feed force for cermets is usually more than that for carbides except at a depth of cut of 0.3 mm. Carbide and cermet inserts behave differently with cutting speed from 80 to 100 m/min. There is a slight increment of feed force with feed rate for cermets, though there is a minimal reduction of feed force for carbides in the feed range of 0.1–0.15 mm/rev. A linear trend of feed force may be seen for both inserts with the depth of cut, where the rate of increment is larger for carbides.

Like feed force, the radial force is higher in the case of cermets. It is evident from Fig. 14a, b that with the cutting speed, radial force gets larger for cermets and the effect is reversed for carbides. Radial force rises linearly with the effect of feed and depth of cut for cermet inserts. At the same time, radial force initially increases and then becomes nearly stable for the carbides.

Figure 15a, b confirms that flank wear of carbides is more than that of cermets. Flank wear of the carbides is uniformly rising with the cutting speed. For cermets, with the cutting speed, the wear on the flank surface drops and then increases. Among the feed range of 0.05–0.1 mm/rev, there is a similar nature of the decline in flank wear for both tools. Subsequently, there is a radical decrement in the flank wear of carbide inserts, wherever flank wear of cermets becomes nearly same. The depth of cut does not seem to have a substantial effect on the flank wear of coated cermets, albeit it increases up to the depth of cut 0.2 mm for uncoated carbides.

Workpiece surface temperature developed during the utilization of carbide tools remains higher than that of cermets, which is clear from Fig. 16a, b. Still the temperature at the cutting speed of 80 m/min is quite closer for both the inserts. There is a negligible alteration in workpiece surface temperature with feed rate, while carbide is considered. A slight fall in temperature occurs with the increase in feed while machining with coated cermet. The temperature of the specimen increases with the depth of cut in the entire range from 0.1 to 0.3 mm in the case of coated cermet, whereas in the case of carbides it initially falls and then rises.

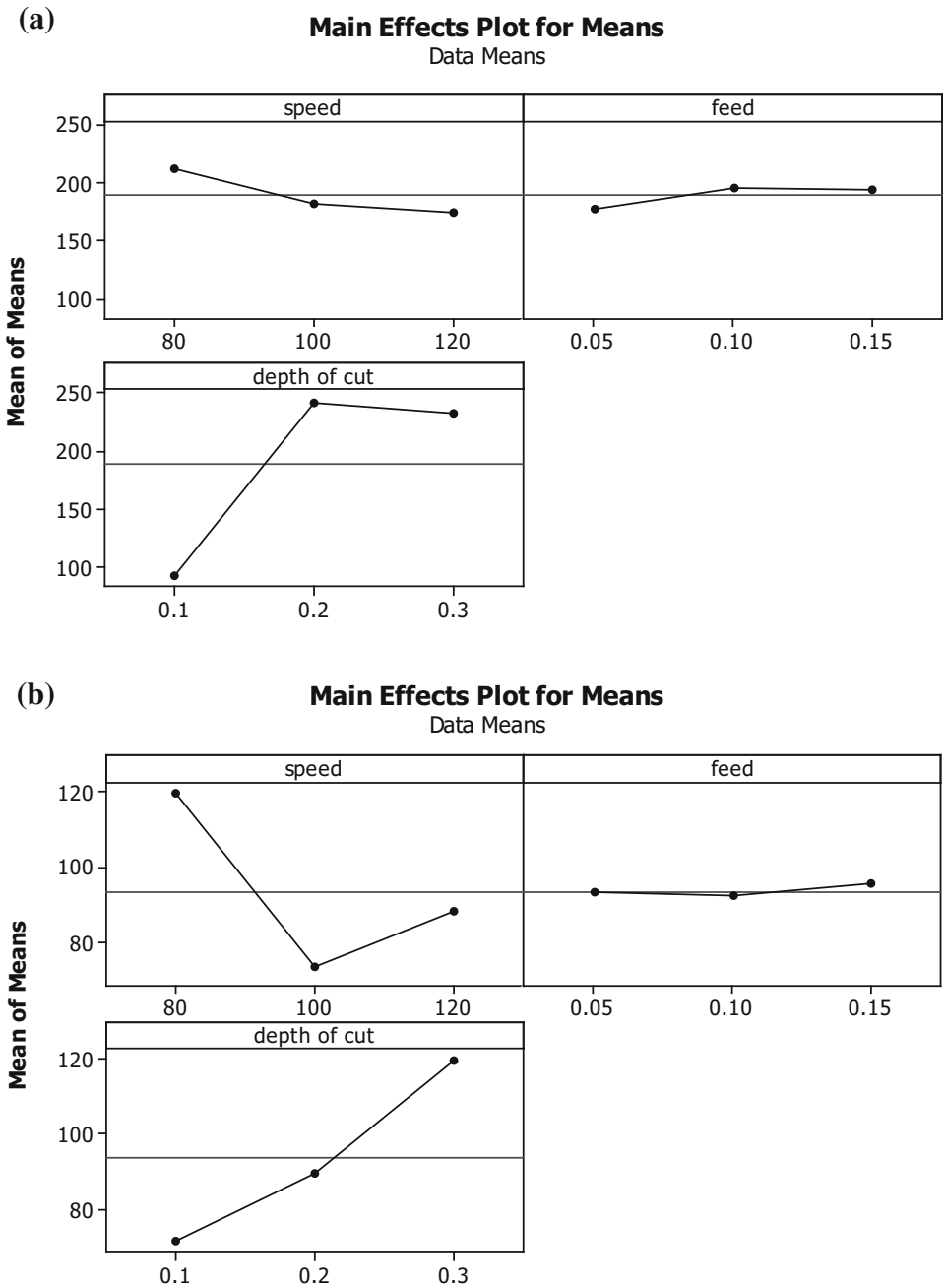

Fig. 12 **a** Main effect plots for cutting force (uncoated carbide). **b** Main effect plots for cutting force (coated cermet)

3.4 Thermal Analysis

According to Davim [1], a non-dimensional entity referred to as Peclet number is useful to study the impact of heat energy in hard machining. It is expressed in terms of cutting speed v, feed f, and thermal diffusivity α of test material as

$$Pe = (v \times f)/\alpha$$

Cutting parameters like cutting speed and feed have supremacy over thermal properties of the work material in influencing the temperature when $Pe > 10$. If $Pe < 10$, thermal properties of the specimen are predominant over cutting parameters. The value of thermal diffusivity of AISI 4340 steel is calculated to be 1.181×10^{-5} m^2/s.

It can be concluded from Table 18 that Peclet number Pe is less than 10 only when feed value is 0.05 mm/rev; otherwise, Pe goes higher than 10. So, the machining parameters are found to have a predominant effect compared to thermal properties of the specimen in the present work.

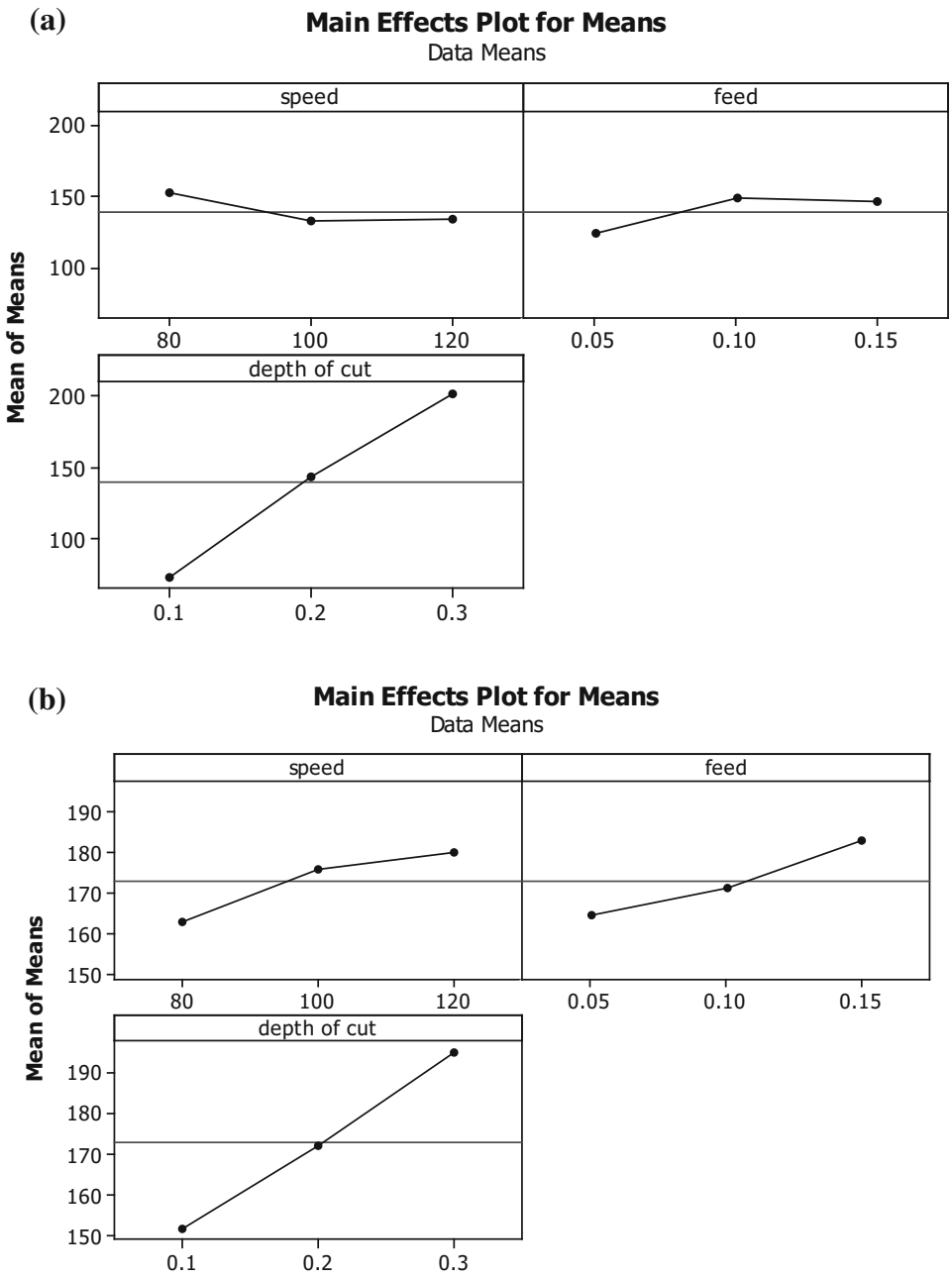

Fig. 13 **a** Main effect plots for feed force (uncoated carbide). **b** Main effect plots for feed force (coated cermet)

3.4.1 Effect of Chip Pattern on Temperature

Machining with carbide inserts created chips of light golden shading in this work, and it is of the helical continuous type as shown in Fig. 17a–d.

This type of color of the chip may be because the heat generated due to friction between insert and work material is not getting removed sufficiently. The retained heat is responsible for higher cutting temperature and lower tool life. On the other hand, the pale blue-colored chips are produced in machining with cermet inserts as shown in Fig. 18a–d. The pale blue color is obtained because an adequate amount of heat is getting expelled from the workpiece.

A lower temperature is observed with cermets as compared with carbides in machining AISI 4340 steel. Cutting speed is the main factor for heat generation in any machining operation. From Fig. 16a, b, it is verified that in the event of both carbide and cermet inserts, the temperature is increasing with cutting speed. This is because, at higher cutting speed, sufficient time is not available for the heat transfer from the work piece to the surroundings.

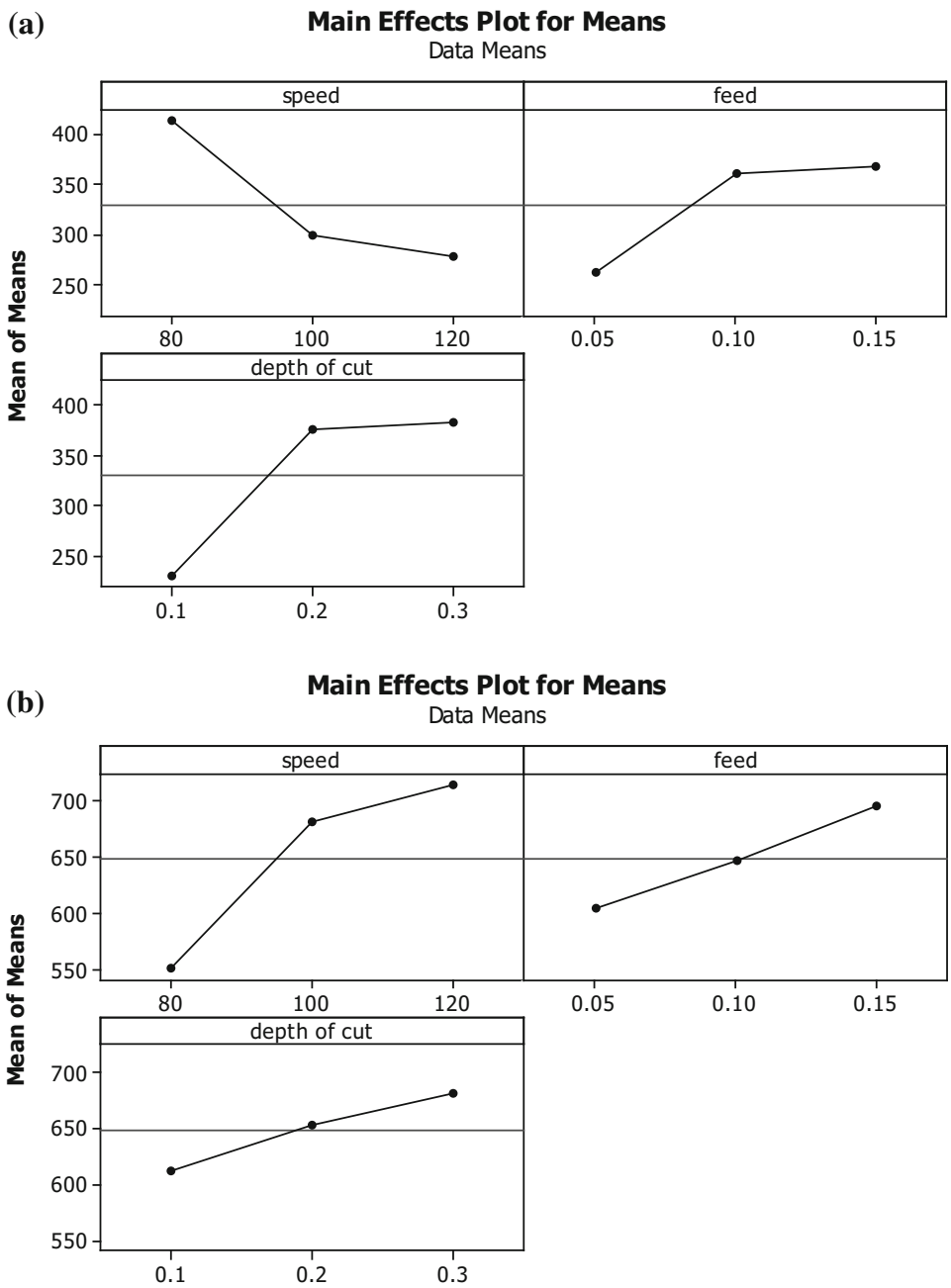

Fig. 14 **a** Main effect plots for radial force (uncoated carbide). **b** Main effect plots for radial force (coated cermet)

3.5 Study on Machining Forces

The insert geometry has a great effect on the machining forces in turning operation. A square insert offers higher cutting force contrasted with rhombic insert. The square insert with a point angle of 90° is robust and tougher than diamond- or rhombic-shaped insert having 80° point angle. Hence, it produces excessive cutting force during machining and consumes additional cutting power.

As carbide insert has higher point angle, the larger portion of the cutting tool is in contact with the workpiece. This creates higher machining forces and work piece temperature as observed in Figs. 12a and 16a. Because of higher machining forces and temperature, both mechanical and thermal loads are dominating on carbide inserts. Later on, edge depression is formed resulting in crest and trough arrangement on the flank surface of this insert because of plastic deformation. Consequently, carbide inserts get worn out to a higher extent compared to cermet and, therefore, require higher machining forces.

The entering or approach angle of carbides and cermets is 75° and 95°, respectively, because of their respective tool holders. Because of lower approach angle, vibration during cutting with carbides is observed to be higher than that with

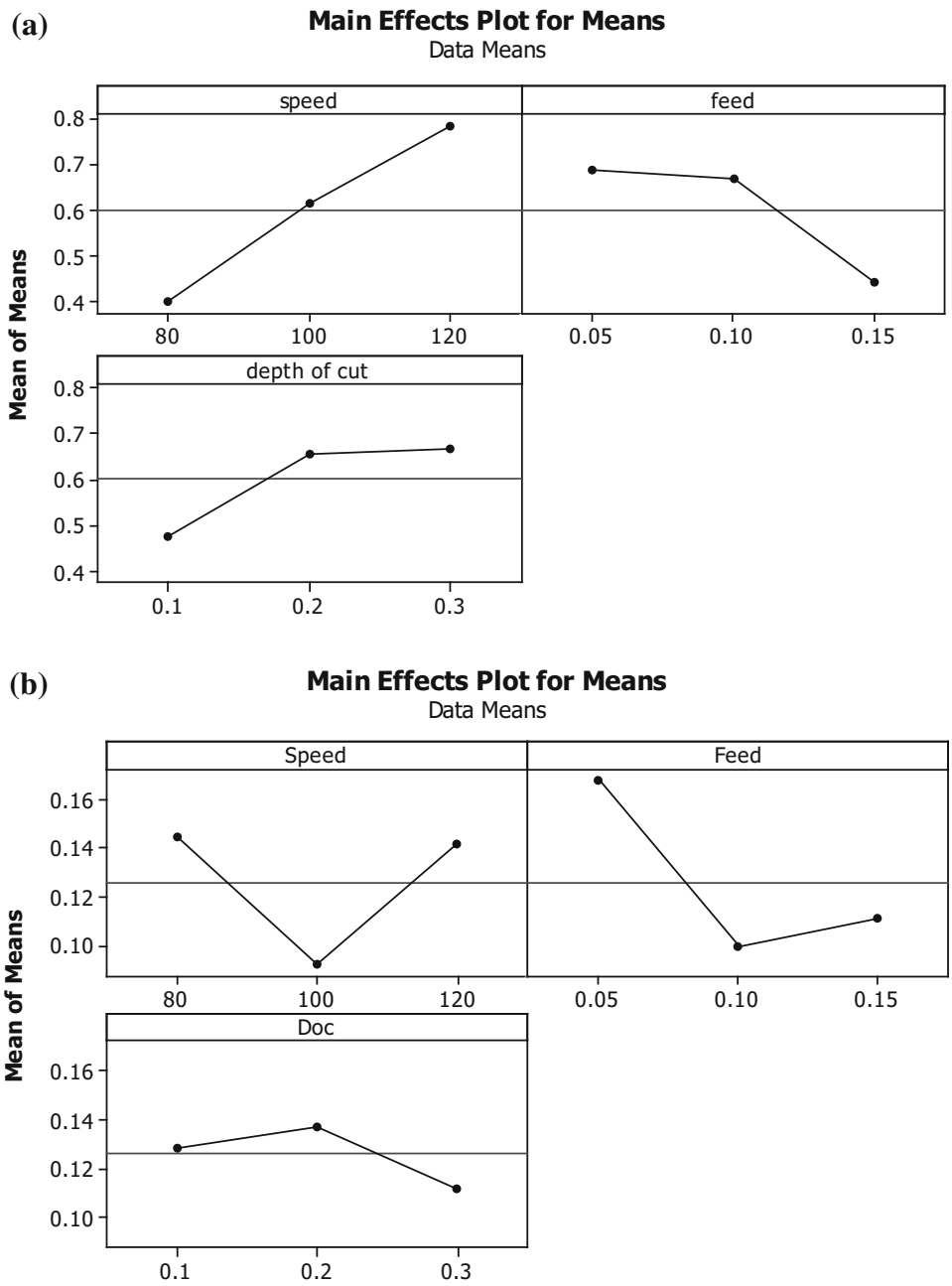

Fig. 15 **a** Main effect plots for flank wear (uncoated carbide). **b** Main effect plots for flank wear (coated cermet)

cermets. As a result, both cutting force and flank wear are seen to be higher for carbides. Consequently, a higher temperature is produced.

Because of the spring back effect of work material, the radial force is dominating over cutting force for both inserts. This also results in higher flank wear, and therefore, both radial and tangential forces become higher.

Tungsten carbide present in uncoated carbide tool is harder than titanium-coated cermet due to its dense structure. As a result, the radial force observed for cermets is more than that for carbides.

3.6 Effects of Chip Breaker Geometry

The inserts used in the present work have two varieties of chip breaker geometry. The uncoated carbide inserts have no specific type of chip breaker geometry; however, coated cermets have the fine finishing type of chip breaker geometry. Controlled contact length exists within the middle of the chip and insert. This resulted in less tool wear in cermets. Thus, higher heat transfer to the chip took place, making the chip blue shaded. This is responsible for decreasing specimen temperature and cutting force for coated cermets. Crater wear of the cermet inserts was less as an aftereffect of the

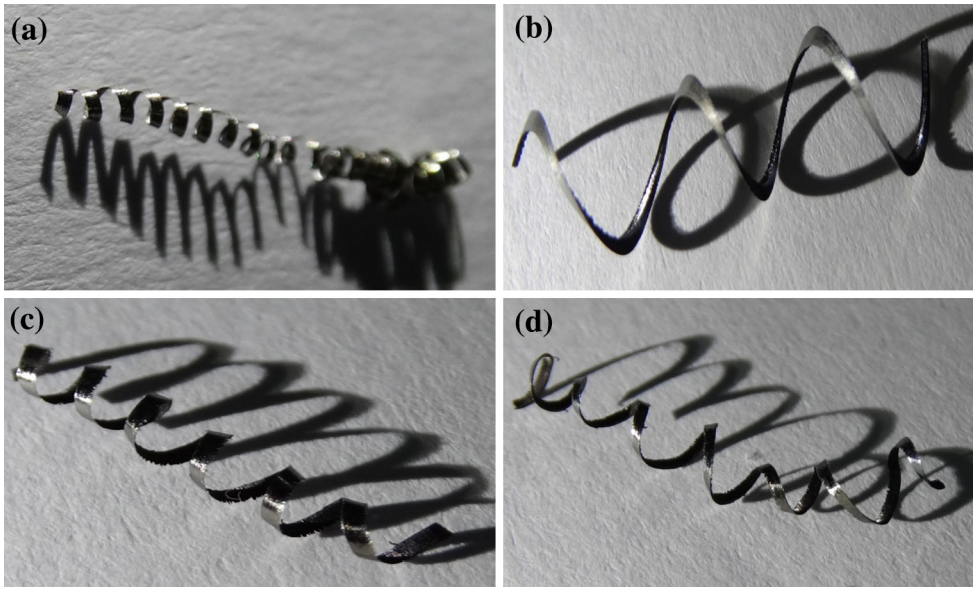

Fig. 16 **a** Main effect plots for specimen temperature (uncoated carbide). **b** Main effect plots for specimen temperature (coated cermet)

Table 18 Peclet number of both inserts

Run no	Peclet no. of uncoated carbide	Peclet no. of coated cermet
1	5.535	5.052
2	11.134	10.084
3	16.360	14.898
4	6.481	5.890
5	12.861	11.670
6	18.926	17.288
7	7.307	6.676
8	14.460	13.182
9	21.452	19.633

vicinity of chip breaker geometry. However, crater wear on carbides is found to be higher as shown in Fig. 21.

3.7 Tool Wear Analysis

In the present study, varieties of the tool wear like crater and flank wear, chipping, built-up edge formation, notch, plastic deformation, chip hammering, development of crest, and trough are seen as discussed below.

Flank wear occurs because of abrasion of the flank face of the cutting tool with the hard constituents like inclusions present in the workpiece due to heat treatment. In this kind of wear, initially coating breaks off and then it gradually affects the substrate material. Flank wear is usually higher at higher cutting speed in case of low wear-resistant grades of inserts. Flank wear measurements in both uncoated carbide and coated cermet are shown in Fig. 19a, b. SEM image of flank wear in coated cermet insert is shown in Fig. 20.

Crater wear is limited to the rake side of the insert. It is because of diffusion, decay, abrasion, and adhesion between the workpiece material and cutting tool. It is enhanced by the tool material and improper chip breaker geometry. Therefore, crater wear is observed to be higher in uncoated carbides. Hard and hot chips break down the binder and disintegrate the substrate in crater wear.

Plastic deformation takes place when the cutting tool softens because of mechanical and thermal over-burdening. It happens when the cutting temperature is too high for the insert to withstand. The shape of insert gets distorted due to thermal softening of binder material, and this subsequently results in depression of cutting edge. It occurs when machining is carried out at high cutting speed and high feed without using any cutting fluid. The SEM image in Fig. 21 shows the crater wear and plastic deformation of uncoated carbide.

Chipping is a kind of flank wear which occurs because of local stress concentration, hard microinclusions exhibit in the workpiece and vibration in machining setup. Vibration and built-up edge cause the local stress concentration in machining. High velocity and low feed escalate chipping phenomenon which can be seen in Figs. 22 and 23.

The mechanism of built-up edge formation is one type of material adhesion which takes place because of pressure welding of the hard chip to the tool rake face. This pressure welding is due to high pressure and low temperature. When the built-up edge breaks, it takes away bits of the coating and substrate material along with it. This phenomenon is often observed during machining with an insert with negative rake angle at low cutting speed and low feed. Figures 24 and 25 show the images of built-up edges formed on carbide insert and cermet insert, respectively.

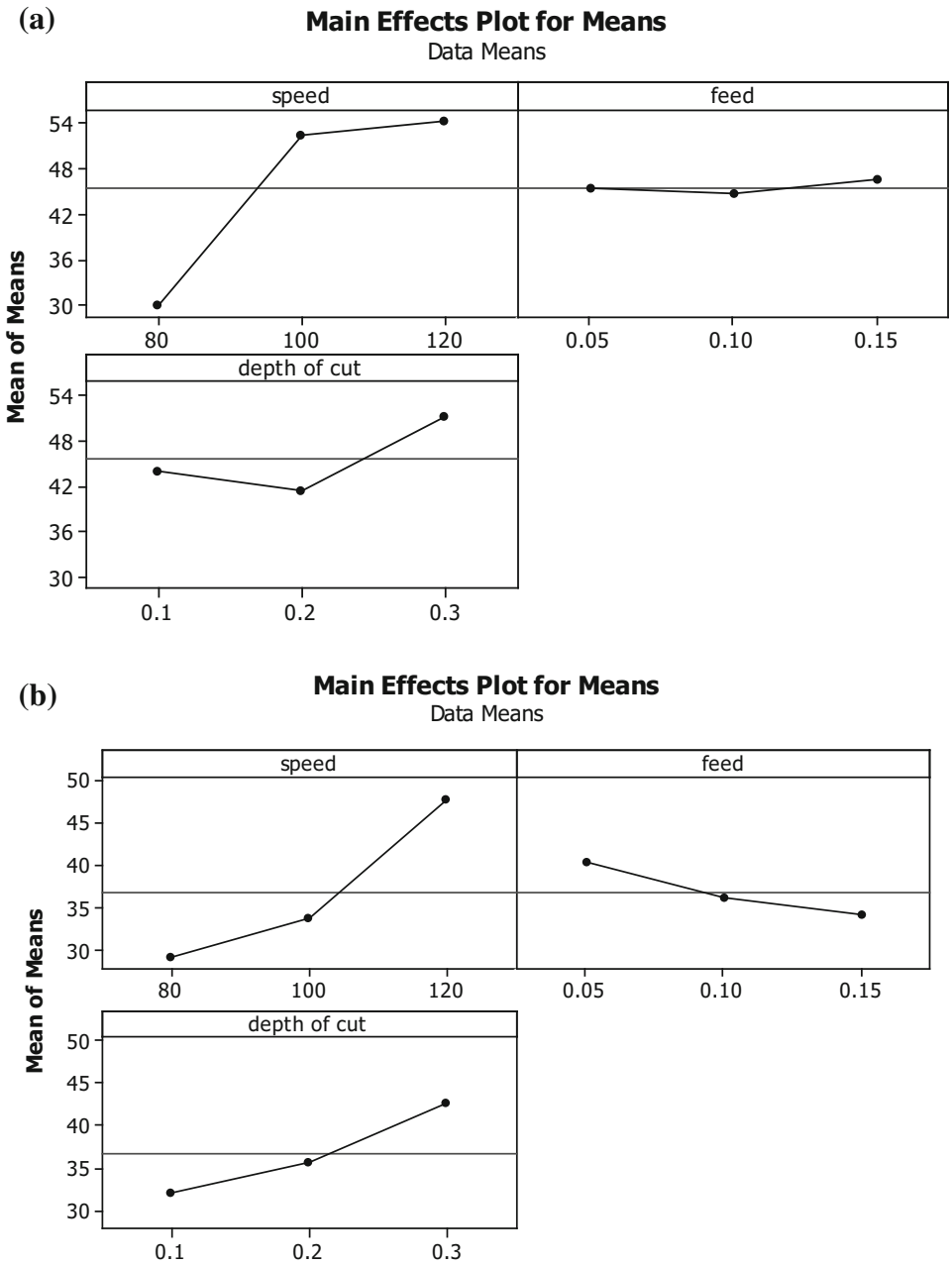

Fig. 17 **a–d** Chips produced with uncoated carbide insert

Notching is a sort of flank wear which is formed at the cutting edge. It generally depends on oxidation of machining surface, local stress fixation at the flank face, hard microincorporation in workpiece, and surface hardening of the workpiece in the previous experimental runs. Notch wear occurs during machining of sticky materials with inserts having high negative rake and approach angles at high cutting speed and feed. Notch wear and chipping of coated cermet can be seen in its SEM image as shown in Fig. 26.

Chip hammering is a kind of abrasive wear which occurs when the chip crashes into the cutting edge and harms it. It usually occurs when long and continuous types of chip are produced during hard machining. Other factors like high feed, high depth of cut, high approach angle, and improper chip breaker geometry also contribute toward this type of wear. This phenomenon is shown in Fig. 27.

Due to heat treatment of steel, the martensitic structure is developed which forms hard inclusions. Because of this, the material is expelled from the flank surface when tool moves over the workpiece. This creates a pattern of peak and trough on the flank surface as shown in Fig. 28. Titanium-coated cermet has a superior crack resistance than that of tungsten carbide. Therefore, this type of wear was not found in titanium-coated cermet inserts.

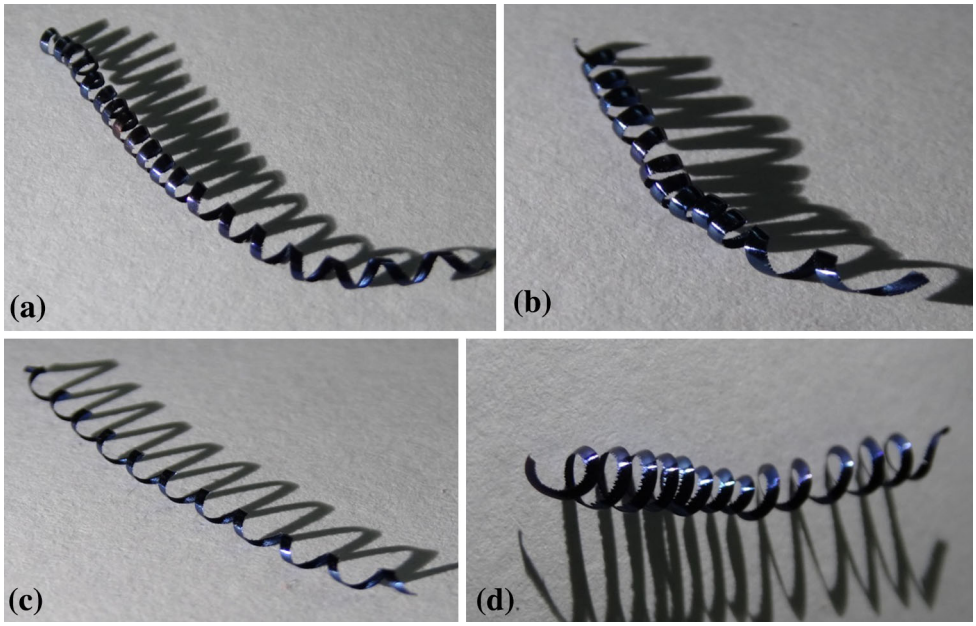

Fig. 18 **a–d** Chips produced with coated cermet insert

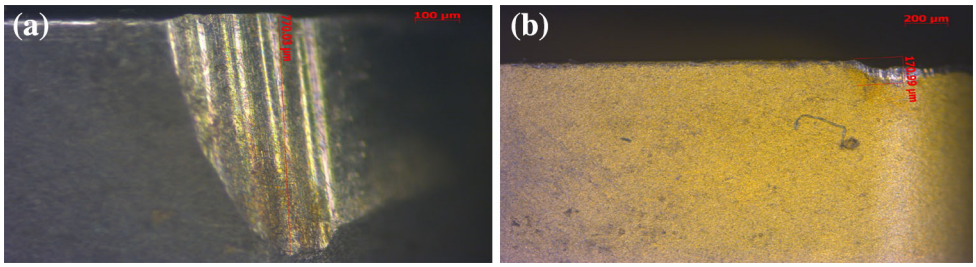

Fig. 19 Flank wear measurement. **a** Uncoated carbide. **b** Coated cermet

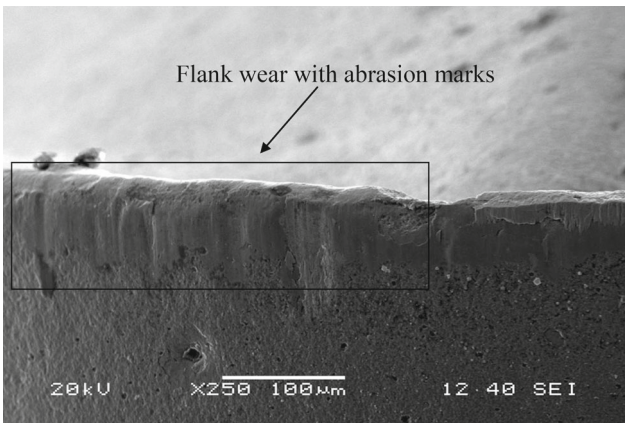

Fig. 20 SEM image of flank wear in coated cermet

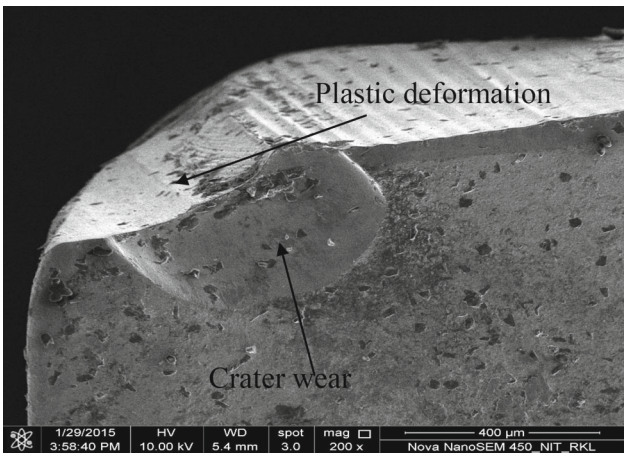

Fig. 21 SEM image of crater wear and plastic deformation in uncoated carbide

The uncoated carbide contains 83 % tungsten carbide and 5.40 % cobalt. Cobalt acts as a binding material. The grain structure of carbide inserts was measured with the help of an optical microscope, and it is found to be in the range of 2.1–3.4 micron. This indicates that its grain structure is of medium coarse type. However, the cermets are found to have a comparatively finer grain structure and thus exhibit longer tool life.

3.7.1 Effect of Coating on Tool Life

Different types of coatings like titanium nitride, titanium carbon nitride, titanium aluminum nitride, zirconium nitride, and diamond coating are often required for the upgradation of tool life. These coatings could be applied either by PVD

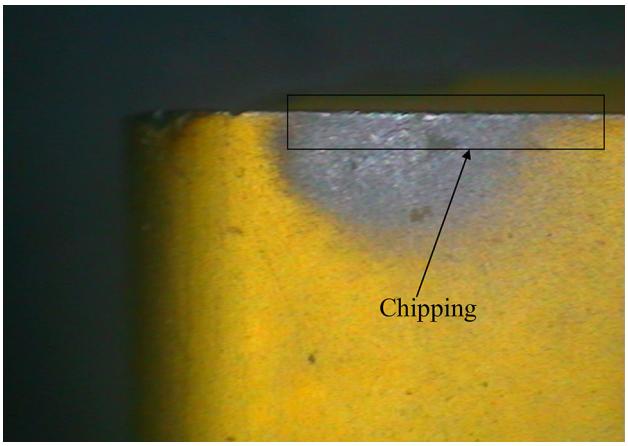

Fig. 22 Chipping in coated cermet

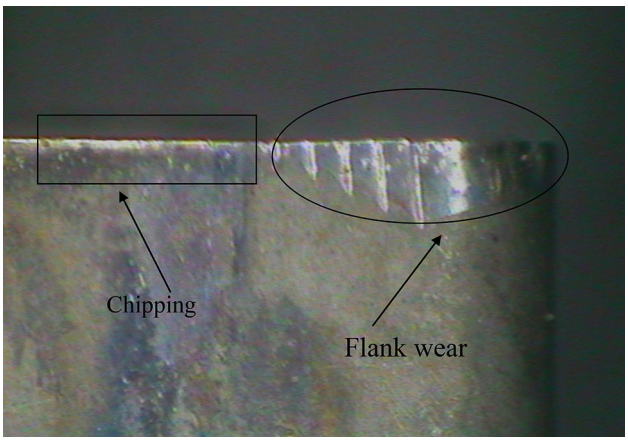

Fig. 23 Chipping in uncoated carbide

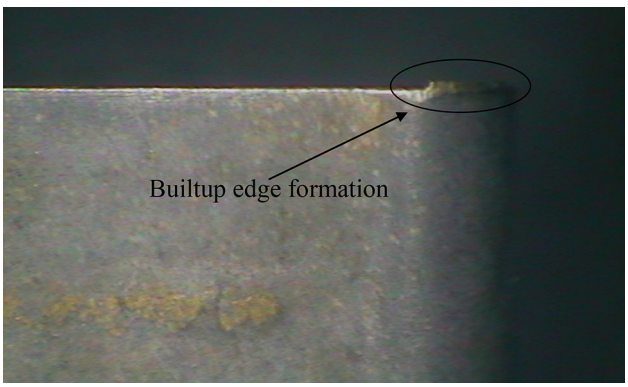

Fig. 24 Built-up edge formation in uncoated carbide

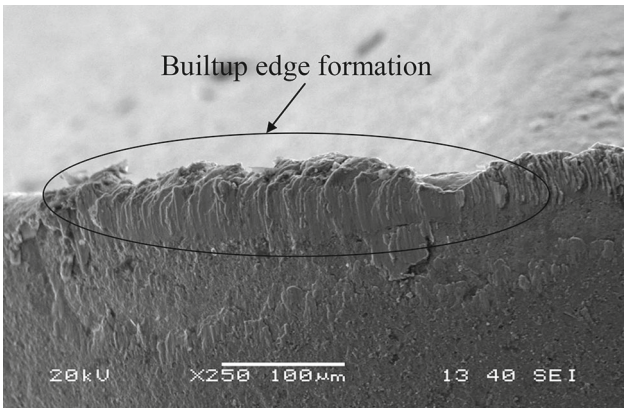

Fig. 25 SEM image of built-up edge formation in coated cermet

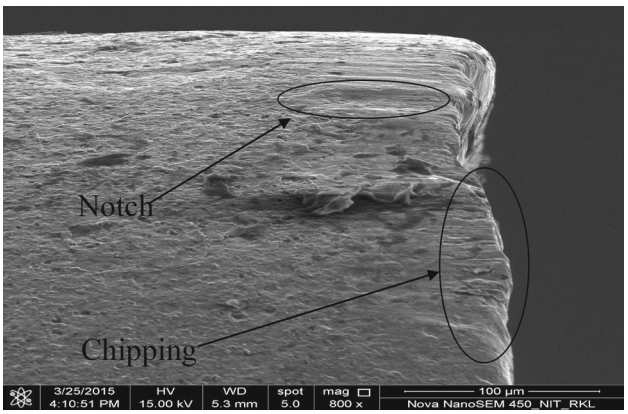

Fig. 26 SEM image of notch wear and chipping in coated cermet

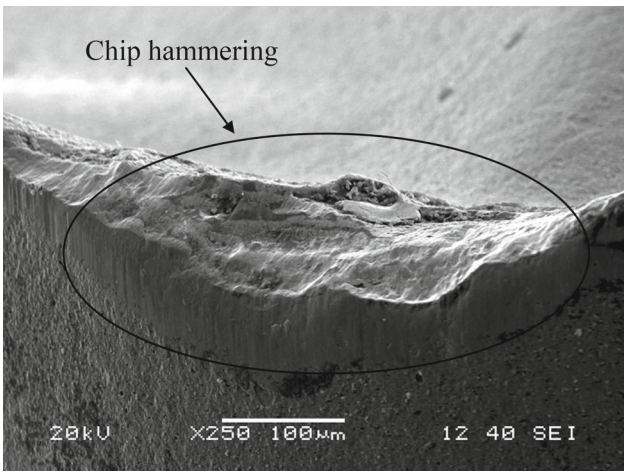

Fig. 27 SEM image of chip hammering and flank wear in uncoated carbide

or by CVD technique. Nonetheless, the thickness is the most important criteria of the coating. Hard and brittle inserts often fail if the coating thickness is high. The cermet inserts used in the present work have a coating thickness of 2–3 µm.

Coating of TiN offers higher resistance to abrasive wear by restricting the built-up edge formation. In addition, it does not allow sticking of the workpiece to the cutting inserts. In conjunction with these, crater wear is constrained and there is an increase in tool life. TiN coating will likewise bring down the coefficient of friction of the insert surface and thereby reduces the machining force and temperature. Also, TiN coatings play an important role when the temperature during machining is

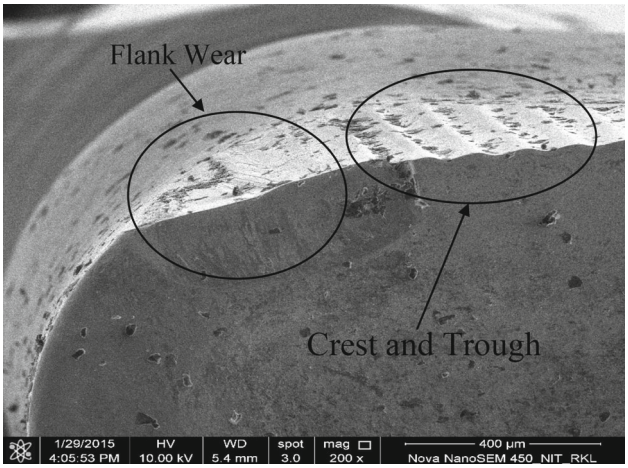

Fig. 28 Crest and trough formation in uncoated carbide

high. It keeps up the chemical stability of the insert at high temperature. In addition, it opposes the oxidation and diffusion. TiCN coating provides the insert with good adhesion and bonding strength. As a result, tool wear of coated cermets and the corresponding workpiece surface temperature were observed to be less than that of uncoated carbides.

Carbide inserts are weaker because of the absence of the coating. Therefore, they experience high progressive wear created by cobalt binder dissemination and also the disintegration of free tungsten carbide stage and complex carbide particles.

4 Conclusions

The following conclusions are drawn out of the results obtained from the current work:

1. Coated cermets experienced a lower cutting force, lower flank wear, and lower workpiece surface temperature but higher feed force and higher radial force compared to uncoated carbides.
2. The depth of cut was the most important parameter for feed force and radial force in case of both coated cermets and uncoated carbide, whereas cutting speed was most significant only for uncoated carbides. Nevertheless, for cermets, cutting force and work piece temperature were found to be significantly affected by cutting speed. Flank wear of both carbides and cermets was mainly influenced by cutting speed and feed.
3. The coating helps in improvement of the performance of the cermet inserts. As a result, tool wear, cutting force, and temperature are less when coated cermets are used instead of uncoated carbides.
4. Peclet number primarily varies with feed and not that much with cutting speed.
5. Chips with serrations are found while machining 4340 hardened alloy steel using carbides and cermets.
6. Flank wear is the prevailing type of wear in case of both types of inserts. Distinctive kinds of flank wear, viz., chipping and notching, were observed.

Acknowledgments We are grateful to the Ministry of Human Resource and Development, Govt. of India, for the financial assistance and research facilities provided at NIT Rourkela, Odisha, for the purpose of experiments and measurements.

References

1. Davim, J.P.: Machining of Hard Materials. Springer, Berlin (2011)
2. Astakhov, V.P.; Joksch, S.: Metalworking Fluids (MWFs) for Cutting and Grinding. Woodhead Publishing Limited, Cambridge (2012)
3. Pal, A. et al.: Machinability assessment through experimental investigation during hard and soft turning of hardened steel. Procedia Mater. Sci. **6**, 80–91 (2014)
4. Suresh, R. et al.: Some studies on hard turning of AISI 4340 steel using multilayer coated carbide tool. Measurement **45**(7), 1872–1884 (2012)
5. Phillip Selvaraj, D. et al.: Optimization of surface roughness, cutting force and tool wear of nitrogen alloyed duplex stainless steel in a dry turning process using Taguchi method. Measurement **49**, 205–215 (2014)
6. Quazi, T.; More, P.G.: Optimization of turning parameters such as speed rate, feed rate, depth of cut for surface roughness by Taguchi method. Asian J. Eng. Technol. Innov. **02**(02), 05–24 (2014)
7. Sahoo, A.K.; Sahoo, B.: Performance studies of multilayer hard surface coatings (TiN/TiCN/Al_2O_3/TiN) of indexable carbide inserts in hard machining: part-I (an experimental approach). Measurement **46**, 2854–2867 (2013)
8. Adesta, E.Y.T.; Riza, M.: Tool wear and surface finish investigation in high speed turning using cermet insert by applying negative rake angles. Eur. J. Sci. Res. **38**(2), 180–188 (2009)
9. Chinchanikar, S.; Choudhury, S.K.: Evaluation of chip-tool interface temperature: effect of tool coating and cutting parameters during turning hardened AISI 4340 steel. Procedia Mater. Sci. **6**, 996–1005 (2014)
10. Chinchanikar, S.; Choudhury, S.K.: Machining of hardened steel—experimental investigations, performance modeling and cooling techniques: a review. Int. J. Mach. Tools Manuf. **89**, 95–109 (2015)
11. Khan, A.A.; Hajjaj, S.S.: Capabilities of cermet tools for high speed machining of austenitic stainless steel. J. Appl. Sci. **6**(4), 779–784 (2006)
12. Noordin, M.Y. et al.: Dry turning of tempered martensitic stainless tool steel using coated cermet and coated carbide tools. J. Mater. Process. Technol. **185**, 83–90 (2007)
13. Ghani, J.A. et al.: Wear mechanism of TiN coated carbide and uncoated cermets tools at high cutting speed applications. J. Mater. Process. Technol. **153–154**, 1067–1073 (2004)
14. Ozakan, M.T. et al.: Experimental design and artificial neural network model for turning the 50CrV4 (SAE 6150) alloy using coated carbide/cermet cutting tools. Mater. Technol. **48**, 227–236 (2014)
15. Thoors, H. et al.: Study of some active wear mechanisms in a titanium-based cermet when machining steels. Wear **162–164**, 1–11 (1993)

16. Sert, H. et al.: Wear behavior of PVD TiAlN, CVD TiN coated, and cermet cutting tools. Tribol. Ind. **27**, 3–9 (2005)
17. Chen, X. et al.: Cutting performance and wear characteristics of Ti(C, N)-based cermet tool in machining hardened steel. Int. J. Refract. Met. Hard Mater. **52**, 143–150 (2015)
18. Dosbaeva, G.K. et al.: Cutting temperature effect on PCBN and CVD coated carbide tools in hard turning of D2 tool steel. Int. J. Refract. Met. Hard Mater. **50**, 1–8 (2015)
19. Fnides, B. et al.: Tool life evaluation of cutting materials in hard turning of AISI H11. Estonian J. Eng. **19**(2), 143–151 (2013)
20. Shalaby, M.A. et al.: Wear mechanisms of several cutting tool materials in hard turning of high carbon–chromium tool steel. Tribol. Int. **70**, 148–154 (2014)
21. Hessainia, Z. et al.: On the prediction of surface roughness in the hard turning based on cutting parameters and tool vibrations. Measurement **46**, 1671–1681 (2013)
22. D' Errico, G.E. et al.: Influences of PVD coatings on cermet tool life in continuous and interrupted turning. J. Mater. Process. Technol. **78**, 53–58 (1998)
23. Rajabi, A. et al.: Development and application of tool wear: a review of the characterization of TiC-based cermets with different binders. Chem. Eng. J. **255**, 445–452 (2014)